Molecular Structures and FT-Raman Spectroscopy of Luminescent Niobium and Tantalum Arylimido Compounds

Kurt S. Heinselman, Vincent M. Miskowski, Steven J. Geib, Louis C. Wang,† and Michael D. Hopkins*

Department of Chemistry, University of Pittsburgh, Pittsburgh, Pennsylvania 15260

Received April 29, 1997[⊗]

Metal−imido compounds of the type *mer-cis*-M(NAr*)X_3L_2 (M = Nb, Ta; Ar* = 2,6-diisopropylphenyl; X = Cl, Br; L_2 = $MeOCH_2CH_2OMe$ (dme), $Me_2NCH_2CH_2NMe_2$ (tmeda), $(C_4H_8O)_2$ ($(thf)_2$), $(C_5H_5N)_2$ ($(py)_2$)) have been synthesized and characterized. The compounds Ta(NAr*)Cl_3(dme) (**1**), Ta(NAr*)Cl_3(tmeda) (**4**), Ta(NAr*)-Br_3(tmeda) (**6**), and Nb(NAr*)Cl_3(dme) (**7**) were studied by single-crystal X-ray diffraction. The M≡N bond lengths (M = Ta, 1.771(6)−1.785(6) Å; M = Nb, 1.746(4) Å) and nearly linear M−N−C linkages (>174°) are characteristic of a formal metal−nitrogen triple bond. With the exception of the M≡N bond distance, which is 0.025 Å shorter for **7** than for **1**, the structure of the MNAr* fragment is insensitive to the natures of M, X, and L. These four compounds and the derivatives Ta(NAr*)$Cl_3(py)_2$ (**2**), Ta(NAr*)$Cl_3(thf)_2$ (**3**), and Ta(NAr*)Br_3-(dme) (**5**) were additionally studied by FT-Raman spectroscopy. The low-frequency regions (≤600 cm^{-1}) of the FT-Raman spectra of **1**−**7** and of difference spectra of pairs of chloride/bromide and niobium/tantalum compounds exhibit bands attributable to M−X stretching modes (X = Cl, 250−360 cm^{-1}; X = Br, 180−220 cm^{-1}) and bending modes (X = Cl, 160−180 cm^{-1}; X = Br, 120 cm^{-1}); analogous M−L modes could not be identified. In the region 900−1600 cm^{-1}, five bands associated with the MNAr* fragment are observed. Two bands, at *ca.* 995 (ν_5) and 1350 cm^{-1} (ν_3), exhibit strong shifts as a function of the metal and are assigned to symmetric and antisymmetric combinations of the nominal ν(M≡N) and ν(N−C) oscillators, respectively; the ν(N−C) mode correlates to mode 13 of benzene and is intrinsically strongly mixed with Ar* internal modes. Two bands at *ca.* 1300 (ν_4) and 1430 cm^{-1} (ν_2) also shift upon metal substitution, indicating that they, too, arise from modes that contain some ν(M≡N) character; they correlate to modes 9a and 19a of benzene, respectively. A fifth band, at *ca.* 1585 cm^{-1} (ν_1), is assigned to Ar*-localized mode 8a. Bands ν_1−ν_4 exhibit preresonance enhancement from a [π(M≡NAr*) → π*(M≡NAr*)] electronic transition. The implications of these results for the excited-state properties of the compounds are discussed.

Introduction

Metal−imido complexes of the type M(≡NR)X_3L_2 (M = Nb, Ta; R = aryl, alkyl; X = halide; L = neutral σ donor)[1,2] constitute the most extensive class of chromophores that exhibit emission from ligand-to-metal charge-transfer excited states in fluid solution at room temperature.[3−7] Work in our laboratory on arylimido derivatives of the type M(NAr*)X_3L_2 (Ar* = 2,6-diisopropylphenyl; Chart 1),[1] the first examples of which were synthesized by Wigley and co-workers,[8] established that the emission is attributable to the [π(M≡NAr*) ← d_{xy}] orbital transition. Two observations support this assignment. First, the energies of the emission bands and corresponding absorption bands are only slightly dependent on the natures of X and L, as expected for a transition between an orbital that is localized on the MNAr* fragment (π(M≡NAr*)) and a metal-centered orbital that has only weak X, and essentially no L, character (d_{xy}). Second, the emission bands of these compounds at 13 K exhibit a 1000−1100 cm^{-1} vibronic progression that is most logically attributable to a mode (or to a set of modes with similar frequencies) localized within the MNAr* unit; MNAr* modes with M≡N stretching character should be vibronically active because the formal M≡N bond order decreases from 3 to $2^1/_2$ in the [π(M≡NAr*) → d_{xy}] excited state. To provide further support for these lines of evidence, we have undertaken X-ray crystallographic and vibrational-spectroscopic studies of M(NAr*)-X_3L_2 complexes with the specific aims of determining the influence of M, X, and L on the structure of the MNAr* fragment and of assigning the vibrational modes of this unit that possess appreciable ν(M≡N) stretching character.

Chart 1

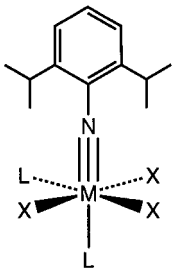

M	X	L_2	
Ta	Cl	dme	**1**
Ta	Cl	$(py)_2$	**2**
Ta	Cl	$(thf)_2$	**3**
Ta	Cl	tmeda	**4**
Ta	Br	dme	**5**
Ta	Br	tmeda	**6**
Nb	Cl	dme	**7**

† Address: Applied Detector Corp., 2325 E. McKinley Ave., Fresno, CA 93703.

⊗ Abstract published in *Advance ACS Abstracts,* October 1, 1997.

(1) Heinselman, K. S.; Hopkins, M. D. *J. Am. Chem. Soc.* **1995**, *117*, 12340−12341.
(2) Williams, D. S.; Thompson, D. W.; Korolev, A. V. *J. Am. Chem. Soc.* **1996**, *118*, 6526−6527.
(3) Lee, Y. F.; Kirchhoff, J. R. *J. Am. Chem. Soc.* **1994**, *116*, 3599−3600.
(4) (a) Pfennig, B. W.; Thompson, M. E.; Bocarsly, A. B. *Organometallics* **1993**, *12*, 649−655. (b) Pfennig, B. W.; Thompson, M. E.; Bocarsly, A. B. *J. Am. Chem. Soc.* **1989**, *111*, 8947−8948.
(5) Thorn, D. L.; Harlow, R. L. *Inorg. Chem.* **1992**, *31*, 3917−3923.
(6) Paulson, S.; Sullivan, B. P.; Caspar, J. V. *J. Am. Chem. Soc.* **1992**, *114*, 6905−6906.
(7) Bandy, J. A.; Cloke, F. G. N.; Cooper, G.; Day, J. P.; Girling, R. B.; Graham, R. G.; Green, J. C.; Grinter, R.; Perutz, R. N. *J. Am. Chem. Soc.* **1988**, *110*, 5039−5050.
(8) Chao, Y.-W.; Wexler, P. A.; Wigley, D. E. *Inorg. Chem.* **1989**, *28*, 3860−3868.

S0020-1669(97)00494-1 CCC: $14.00

Experimental Section

General Procedures. All compounds were prepared and handled under a nitrogen atmosphere using standard inert-atmosphere glovebox and Schlenk techniques. Solvents were purified as follows: diethyl ether and 1,2-dimethoxyethane (dme) were distilled from potassium benzophenone ketyl; benzene, toluene, and *N*,*N*,*N*′,*N*′-tetramethylethylenediamine (tmeda) were distilled from sodium; pentane was stirred first over a mixture of concentrated sulfuric acid and nitric acid (95:5 v/v) and then over potassium carbonate and distilled from calcium hydride; and benzene-d_6 was stirred over 1:4 Na/K alloy, from which it was distilled under vacuum. The compounds Ta(NAr*)Cl_3(dme) (**1**), Ta(NAr*)$Cl_3(py)_2$ (**2**), Ta(NAr*)$Cl_3(thf)_2$ (**3**), and Ar*NH($SiMe_3$) were prepared according to standard procedures.[8] Other chemicals were of reagent grade or comparable quality and were used as received.

FT-Raman spectra of polycrystalline samples sealed in glass capillaries were recorded at 1 cm^{-1} resolution using a Nicolet model 950 FT-Raman spectrometer (Nd:YVO_4 source, $\lambda = 1064$ nm) fitted with a liquid-nitrogen-cooled germanium-diode detector (Applied Detector Corp. model 403NR). Frequencies were calibrated against an external indene reference. Intensities are corrected for detector response; relative intensities (vs, s, m, w, vw) are normalized to the band at *ca.* 1585 cm^{-1} (s) observed in all spectra. ^{1}H NMR spectra (300.13 MHz) were measured at ambient temperature in C_6D_6 solutions. Elemental analyses were performed by Oneida Research Services, Inc., Whitesboro, NY.

Ta(NAr*)Cl_3(tmeda) (4). To a stirred, room-temperature suspension of $TaCl_5$ (2.90 g, 8.1 mmol) in benzene (100 mL) were successively added dropwise diethyl ether (8 mL) and a mixture of tmeda (2.51 g, 21.6 mmol) and Ar*NH($SiMe_3$) (4.30 g, 17.2 mmol). The reaction mixture was heated to 60 °C for 24 h. After cooling to room temperature, the orange solution was concentrated to 20 mL in vacuo and allowed to stand undisturbed for 48 h. The resulting orange crystals were quickly washed with benzene (2 × 10 mL). Recrystallization from toluene at −30 °C yielded 1.34 g (29%) of analytically pure needlelike crystals, after drying in vacuo. ^{1}H NMR: δ 7.23 (d, 2 H, $^3J_{HH} = 7.7$ Hz, H_{meta}), 6.83 (t, 1 H, $^3J_{HH} = 7.7$ Hz, H_{para}), 4.88 (sep, 2 H, $^3J_{HH} = 6.8$ Hz, C*H*(CH_3)$_2$, 2.53 (s, 6 H, N(C*H*$_3$)$_2$), 2.36 (s, 6 H, N(C*H*$_3$)$_2$), 1.88 (m (AA′BB′), 2 H, NC*H*$_2$), 1.85 (m (AA′BB′), 2 H, NC*H*$_2$), 1.48 (d, 12 H, $^3J_{HH} = 6.8$ Hz, CH(C*H*$_3$)$_2$). Anal. Calcd (found) for $C_{18}H_{33}Cl_3N_3Ta$: C, 37.35 (36.81); H, 5.75 (5.56); N, 7.26 (7.07).

Ta(NAr*)Br_3(dme) (5). To a stirred, room-temperature suspension of $TaBr_5$ (1.74 g, 3.0 mmol) in toluene (15 mL) was added slowly a mixture of dme (3.80 g, 42.2 mmol) and Ar*NH($SiMe_3$) (1.50 g, 6.0 mmol). The reaction mixture was stirred for 24 h, during which the color changed from orange to red-orange and orange microcrystals formed; these were washed with pentane (3 × 3 mL) and dried in vacuo to yield 1.50 g (73%) of crude product. The product was recrystallized from toluene at −30 °C; the resulting orange microcrystals were dried in vacuo. ^{1}H NMR: δ 7.24 (d, 2 H, $^3J_{HH} = 7.7$ Hz, H_{meta}), 6.82 (t, 1 H, $^3J_{HH} = 7.7$ Hz, H_{para}), 4.85 (sep, 2 H, $^3J_{HH} = 6.8$ Hz, C*H*(CH_3)$_2$), 3.55 (s, 3 H, OC*H*$_3$), 3.21 (s, 3 H, OC*H*$_3$), 2.94 (m (AA′BB′), 2 H, OC*H*$_2$), 2.87 (m (AA′BB′), 2 H, OC*H*$_2$), 1.48 (d, 12 H, $^3J_{HH} = 6.9$ Hz, CH(C*H*$_3$)$_2$). Anal. Calcd (found) for $C_{16}H_{27}Br_3NO_2Ta$: C, 28.01 (28.07); H, 3.97 (3.92); N, 2.04 (1.97).

Ta(NAr*)Br_3(tmeda) (6). To a stirred, room-temperature suspension of $TaBr_5$ (2.50 g, 4.3 mmol) in benzene (100 mL) were successively added dropwise diethyl ether (4 mL) and a mixture of tmeda (1.30 g, 11.2 mmol) and Ar*NH($SiMe_3$) (2.15 g, 8.6 mmol). The reaction mixture was heated to 60 °C for 24 h, during which the solid dissolved and the solution darkened. The reaction mixture was allowed to cool to room temperature, concentrated to 20 mL in vacuo, and allowed to stand undisturbed for 48 h. The resulting precipitate was quickly washed with benzene (2 × 10 mL). Recrystallization from toluene at −30 °C was essential to remove a gray-brown impurity and yielded 2.50 g (82%) of needlelike translucent purple-red crystals, after drying in vacuo. ^{1}H NMR: δ 7.27 (d, 2 H, $^3J_{HH} = 7.7$ Hz, H_{meta}), 6.79 (t, 1 H, $^3J_{HH} = 7.7$ Hz, H_{para}), 4.92 (sep, 2 H, $^3J_{HH} = 6.8$ Hz, C*H*(CH_3)$_2$), 2.77 (s, 6 H, N(C*H*$_3$)$_2$), 2.42 (s, 6 H, N(C*H*$_3$)$_2$), 1.98 (m (AA′BB′), 2 H, NC*H*$_2$), 1.94 (m (AA′BB′), 2 H, NC*H*$_2$), 1.47 (d, 12 H, $^3J_{HH} = 6.9$ Hz, CH(C*H*$_3$)$_2$). Anal. Calcd (found) for $C_{18}H_{33}Br_3N_3Ta$: C, 30.36 (30.36); H, 4.67 (4.65); N, 5.90 (5.75).

Nb(NAr*)Cl_3(dme) (7). To a stirred, room-temperature yellow suspension of $NbCl_5$ (1.62 g, 6.0 mmol) in toluene (15 mL) was added slowly a mixture of dme (7.60 g, 84.3 mmol) and Ar*NH($SiMe_3$) (3.00 g, 12.0 mmol). The resulting red-purple solution was stirred for 24 h, during which a purple precipitate formed; this was washed with pentane (3 × 3 mL) and dried in vacuo. The product was recrystallized from toluene at −30 °C to yield 1.60 g (58%) of purple crystals, after drying in vacuo. ^{1}H NMR: δ 7.06 (d, 2 H, $^3J_{HH} = 7.7$ Hz, H_{meta}), 6.89 (t, 1 H, $^3J_{HH} = 7.7$ Hz, H_{para}), 4.86 (sep, 2 H, $^3J_{HH} = 6.8$ Hz, C*H*(CH_3)$_2$), 3.40 (s, 3 H, OC*H*$_3$), 3.15 (s, 3 H, OC*H*$_3$), 2.90 (m (AA′BB′), 2 H, OC*H*$_2$), 2.87 (m (AA′BB′), 2 H, OC*H*$_2$), 1.46 (d, 12 H, $^3J_{HH} = 6.7$ Hz, CH(C*H*$_3$)$_2$). Anal. Calcd (found) for $C_{16}H_{27}Cl_3NO_2Nb$: C, 41.36 (41.53); H, 5.86 (5.70); N, 3.01 (2.86).

Single-Crystal X-ray Diffraction Studies. X-ray crystal structures were determined for Ta(NAr*)Cl_3(dme) (**1**), Ta(NAr*)Cl_3(tmeda) (**4**), Ta(NAr*)Br_3(tmeda) (**6**), and Nb(NAr*)Cl_3(dme) (**7**) using a Siemens P3 diffractometer with graphite-monochromated Mo Kα ($\lambda = 0.710\ 73$ Å) radiation. Crystals were attached to fine glass fibers with Fluorolube and placed in a cold N_2 stream (−65 °C) for data collection. The crystal data and data collection and refinement parameters are given in Table 1. All computer programs used in the data collection and refinements are contained in the Siemens program packages P3 and SHELXTL (version 5.02).

Unit-cell parameters, systematic absences, and axial rotation photographs indicate that Ta(NAr*)Cl_3(tmeda) and Ta(NAr*)Br_3(tmeda) are uniquely assignable to the centrosymmetric space groups *Pbca* and $P2_1/n$, respectively, and that the isomorphous compounds M(NAr*)Cl_3(dme) (M = Nb, Ta) crystallize in either *Pnam* or $Pna2_1$. Noncentrosymmetric space group $Pna2_1$ was chosen on the basis of *E* values and the well-behaved solution and refinement of the structure. For each structure, unit-cell dimensions were derived from least-squares fits of the angular settings of 25 reflections with $21° < 2\theta < 26°$. The data were corrected for absorption using ψ scans. Three standard reflections were monitored every 200 reflections during each data collection to check for decay; the observed decay was <1%.

Each structure was solved via direct methods, which located the positions of the metal and halogen atoms. Remaining non-hydrogen atoms were located from subsequent difference Fourier syntheses and refined anisotropically. Idealized positions were calculated for the hydrogen atoms (d(C−H) = 0.96 Å, $U = 1.2(U_{iso}$ of attached carbon)). Each asymmetric unit consists of a single molecule with no crystallographically imposed symmetry. The chiralities of the crystals of **1** and **7** were established by refinement of Flack's absolute-structure parameter.[9]

Final difference Fourier syntheses showed residual electron density only near M (≤1 Å). Inspection of F_o vs F_c values and trends based upon sin θ, Miller index, or parity group did not indicate any systematic errors in the data.

Results and Discussion

X-ray Diffraction Studies. The molecular structures of Ta(NAr*)Cl_3(dme) (**1**), Ta(NAr*)Cl_3(tmeda) (**4**), Ta(NAr*)Br_3(tmeda) (**6**), and Nb(NAr*)Cl_3(dme) (**7**) are shown in Figures 1−4, respectively, and selected bond distances and bond angles are given in Table 2. All four compounds exhibit the mer-cis stereochemistry expected on the basis of their ^{1}H NMR spectra and from the crystal structure of the closely related compound *mer*-Ta(NPh)$Cl_3(thf)(PEt_3)$,[10] with the three halide ligands occupying equatorial sites relative to the M≡N axis and the chelating dme or tmeda ligands spanning a pair of sites cis and trans to the imido ligand.

The molecular symmetry of the compounds in the solid state is C_1, with the plane of the aryl ring roughly bisecting the X(1)−M−X(2) and X(3)−M−E(cis) axes (where E(cis) is the ligating atom of L cis to the imido ligand);[11] idealized C_s-symmetry configurations result when the plane of the aryl ring contains

(9) Flack, H. D. *Acta Crystallogr.* **1983**, *A39*, 876−881.
(10) Churchill, M. R.; Wasserman, H. J. *Inorg. Chem.* **1982**, *21*, 223−226.
(11) Angles between the least-squares plane of the six aryl-ring carbon atoms and the least-squares planes defined by {M, X(1), X(2), N(1)} and {M, X(3), E(cis), N(1)}: **1**, 52.5, 39.7°; **4**, 15.3, 73.7°; **6**, 40.5, 50.0°; **7**, 52.4, 40.1°.

Table 1. Crystal Data and Data Collection and Refinement Parameters for Ta(NAr*)Cl_3(dme) (**1**), Ta(NAr*)Cl_3(tmeda) (**4**), Ta(NAr*)Br_3(tmeda) (**6**), and Nb(NAr*)Cl_3(dme) (**7**)

	1	**4**	**6**	**7**
		Crystal Data		
empirical formula	$C_{16}H_{27}Cl_3NO_2Ta$	$C_{18}H_{33}Cl_3N_3Ta$	$C_{18}H_{33}Br_3N_3Ta$	$C_{16}H_{27}Cl_3NNbO_2$
fw	552.69	578.77	712.15	464.64
crystal system	orthorhombic	orthorhombic	monoclinic	orthorhombic
space group	*Pna*2_1	*Pbca*	*P*2_1/*n*	*Pna*2_1
Z	4	8	4	4
a, Å	14.430(3)	16.722(14)	10.111(2)	14.494(6)
b, Å	9.813(2)	15.509(13)	14.700(3)	9.819(3)
c, Å	14.370(3)	17.74 (2)	15.931(3)	14.342(4)
β, deg			91.95(3)	
V, Å^3	2034.8(7)	4601(7)	2366.5(8)	2041.1(12)
μ(Mo Kα), mm^{-1}	5.803	5.133	9.717	0.990
D_{calcd}, g cm^{-3}	1.804	1.671	1.999	1.512
F(000)	1080	2288	1360	952
crystal size, mm	0.12 × 0.19 × 0.38	0.41 × 0.36 × 0.36	0.17 × 0.26 × 0.37	0.25 × 0.25 × 0.25
		Data Collection and Refinement Parameters		
2θ limits, deg	5−49	4−48	5−48	5−50
octants	±*h*,+*k*,+*l*	+*h*,+*k*,−*l*	+*h*,+*k*,±*l*	+*h*,±*k*,+*l*
no. of reflns (collec/indep/R_{int})	3262/1670/0.0183	3271/3271/0	3952/3726/0.0961	3623/1871/0.0308
no. of restraints/parameters	1/210	0/244	0/226	1/209
*R*1,[a] w*R*2[b] [$I > 2\sigma(I)$]	0.0183, 0.0396	0.0327, 0.0965	0.0521, 0.1104	0.0235, 0.0522
*R*1,[a] w*R*2[b] (all data)	0.0247, 0.0420	0.0535, 0.1228	0.0908, 0.1290	0.0296, 0.0556
GOF[c] on F^2	0.965	0.835	1.033	1.057
largest diff peak and hole, e Å^{-3}	0.457, −0.403	0.965, −0.861	2.280, −1.217	0.490, −0.288
Flack parameter, *x*	0.01(3)			−0.10(12)
extinction coeff	0.00022(9)	0.00009(9)		

[a] $R1 = \sum||F_o| - |F_c||/\sum|F_o|$. [b] $wR2 = [\sum w(F_o^2 - F_c^2)^2/\sum w(F_o^2)^2]^{1/2}$. [c] GOF $= S = [\sum w(F_o^2 - F_c^2)^2/(n - p)]^{1/2}$.

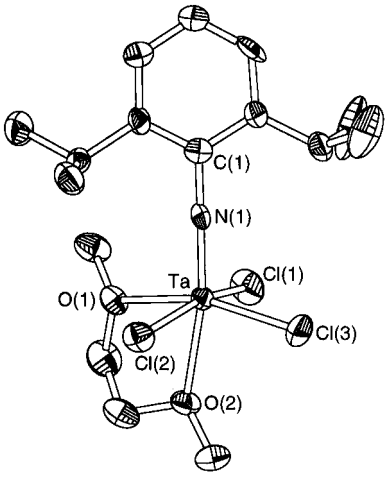

Figure 1. ORTEP representation of Ta(NAr*)Cl_3(dme) (**1**), drawn with 50% probability ellipsoids. For clarity, hydrogen atoms are omitted.

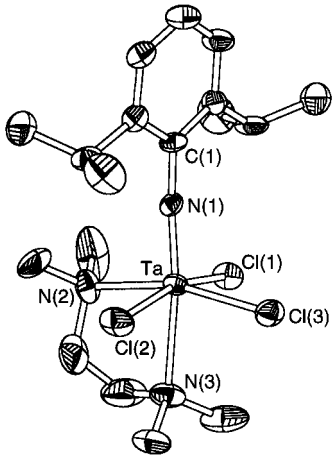

Figure 2. ORTEP representation of Ta(NAr*)Cl_3(tmeda) (**4**), drawn with 50% probability ellipsoids. For clarity, hydrogen atoms are omitted.

either of these axes. The ^{1}H NMR spectra of these compounds are consistent with free rotation of the Ar* ring in solution at room temperature. The metal atoms lie above the approximate equatorial plane formed by X(1), X(2), X(3), and E(cis) ($\angle$(N(1)−M−X) = 95−101°; $\angle$(N(1)−M−E(cis)) = 95−99°). It has been suggested previously that the "steric pressure" exerted by the NAr* ligand upon equatorial ligands is slightly greater than that exerted by NPh, on the basis of a comparison of the structures of *trans-mer*-W(NR)Cl_3(PMe_3)$_2$ (R = Ph, Ar*).[12] There are no obvious structural manifestations of this difference in the present compounds, however; for example, the N(1)−Ta−Cl bond angles of Ta(NAr*)Cl_3(dme) (**1**) are nearly identical to those for Ta(NPh)Cl_3(thf)(PEt_3).[10]

The MNAr* fragments exhibit the standard structural characteristics of high-valent metal−imido complexes.[13,14] The M≡N−C linkages are essentially linear (>174°) and the M≡N bonds are short (Ta, 1.771(6)−1.785(6) Å; Nb, 1.746(4) Å), consistent with a formal metal−nitrogen triple bond. Comparisons among the bond distances and bond angles within the MNAr* units of the tantalum compounds (Table 2) reveal them to be insensitive to the nature of the ancillary ligands (Cl, Br, dme, tmeda); with the exception of the M≡N distance, which is *ca.* 0.03 Å shorter for Nb(NAr*)Cl_3(dme) than for the tantalum compounds (*vide infra*), they are also insensitive to the nature of the metal.

Within the MX_3L_2 fragment, the most notable trends among the metrical data are those that manifest the differing trans influences of the ligands. Specifically, the M−E(cis) bond distances are *ca.* 0.10−0.25 Å shorter than the M−E(trans) bond distances, consistent with the large trans influence of the imido ligand.[15] The M−X bond distances of the mutually trans halides, X(1) and X(2), are statistically indistinguishable in each compound and are independent of L (as judged by comparing

(12) Clark, G. R.; Nielson, A. J.; Rickard, C. E. F. *J. Chem. Soc., Dalton Trans.* **1995**, 1907−1914.
(13) Wigley, D. E. *Prog. Inorg. Chem.* **1994**, *42*, 293−483.
(14) Nugent, W. A.; Mayer, J. M. *Metal-Ligand Multiple Bonds*; Wiley: New York, 1988; Chapter 5.
(15) Lyne, P. D.; Mingos, D. M. P. *J. Organomet. Chem.* **1994**, *478*, 141−151 and references therein.

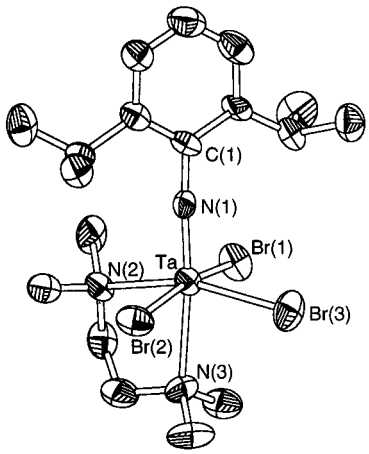

Figure 3. ORTEP representation of Ta(NAr*)Br_3(tmeda) (**6**), drawn with 50% probability ellipsoids. For clarity, hydrogen atoms are omitted.

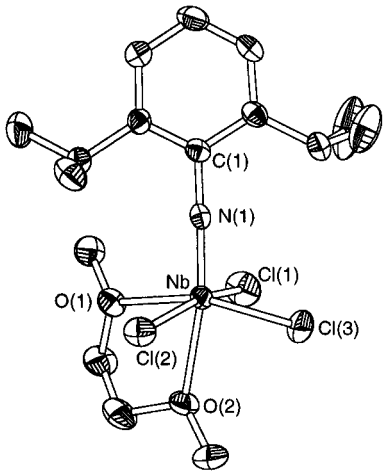

Figure 4. ORTEP representation of Nb(NAr*)Cl_3(dme) (**7**), drawn with 50% probability ellipsoids. For clarity, hydrogen atoms are omitted.

Ta(NAr*)Cl_3(dme) (**1**) and Ta(NAr*)Cl_3(tmeda) (**4**)), while that for X(3), which is trans to E(cis), is shorter than these M−X bonds by 0.004−0.040 Å and is sensitive to L (d(Ta−X(3)) = 2.338(3) Å (**1**), 2.376(2) Å (**4**)). The Ta−Br bond distances of Ta(NAr*)Br_3(tmeda) (**6**) differ from the Ta−Cl bond distances of Ta(NAr*)Cl_3(tmeda) (**4**) approximately by the difference between the ionic radii of bromide and chloride (0.15 Å).[16]

A striking observation is that whereas the M≡N bond distance is 0.025 Å shorter for Nb(NAr*)Cl_3(dme) (**7**) than for analogous Ta(NAr*)Cl_3(dme) (**1**), the M−Cl and M−O bond distances are longer for the niobium compound than for the tantalum derivative (Δd(M−Cl) = 0.012−0.017 Å, Δd(M−O) = 0.022, 0.024 Å; Table 2). The trend in Δd(M−Cl) is consistent with that predicted from the ionic radii for Nb^{5+} (0.069 Å) and Ta^{5+} (0.064 Å),[16] and it is logical that bond distances for weakly bound neutral σ-donor ligands such as dme should follow those for (largely) ionically bound anionic ligands like chloride. The reverse ordering of the M≡N distances, then, must reflect differences in the covalent, triple-bond radii of the metals. An important parameter in this regard is the $d\pi_{xz,yz}/p\pi_{x,y}$ orbital overlap, given that the short M≡N bond distances imply strong M≡N π-bonding; in view of the greater radial extensions of 5d orbitals relative to 4d orbitals, it is reasonable to expect that M≡N π-bonding may optimize at a slightly longer M≡N distance for tantalum than for niobium.

Vibrational Spectroscopy. Interpreting the vibrational spectra of metal−alkylimido and −arylimido complexes, particularly as regards the assignment of the M≡N stretching mode (*vide infra*), is an intrinsically difficult task, which is exacerbated in the case of M(NAr*)X_3L_2 compounds by their complex compositions and lack of symmetry; the M(NAr*)X_3 fragment possesses 96 degrees of vibrational freedom, to which are added those of the two chemically inequivalent L ligands. In view of this spectral congestion, we measured vibrational spectra for **1**−**7** by FT-Raman spectroscopy (λ_{ex} = 1064 nm) instead of by infrared spectroscopy, which has been used almost exclusively in prior studies of metal−imido complexes, because of the standard problem of acquiring spectra for solid-phase samples by the latter method that are free from the effects of optical dispersion (irreproducible base lines and asymmetric line broadening). The FT-Raman spectrum of Ta(NAr*)Cl_3(tmeda) (**4**) presented in Figure 5a is representative of the well-resolved spectra provided by this technique for these compounds. FT-Raman spectroscopic data for **1**−**7** are given in Table 3. For those infrared bands for **1**−**7** that can be clearly resolved, the frequencies typically agree well with those measured by FT-Raman spectroscopy and with those previously reported for **1**−**3**,[8] and there are also obvious similarities to the infrared spectra of related complexes of the type W(NAr*)Cl_3L_2.[17] We are aware of only one previous detailed study of metal−imido complexes by Raman spectroscopy, that being a study by Griffith and co-workers that employed visible-wavelength excitation.[18]

We have not obtained vibrational spectra for ^{15}N-labeled derivatives, which have been used to identify metal−imido vibrational modes in previous studies.[13,18−22] However, comparisons among the spectroscopic data for these complexes, in

Table 2. Selected Bond Distances and Bond Angles for Ta(NAr*)Cl_3(dme) (**1**), Ta(NAr*)Cl_3(tmeda) (**4**), Ta(NAr*)Br_3(tmeda) (**6**), and Nb(NAr*)Cl_3(dme) (**7**)

nuclei[a]	**1**	**4**	**6**	**7**
Bond Distances (Å)				
M−N(1)	1.771(6)	1.785(6)	1.774(10)	1.746(4)
M−X(1)	2.378(2)	2.380(3)	2.549(2)	2.391(1)
M−X(2)	2.376(2)	2.383(2)	2.542(2)	2.390(1)
M−X(3)	2.338(3)	2.376(2)	2.513(2)	2.355(2)
M−E(cis)	2.208(6)	2.325(7)	2.335(10)	2.232(3)
M−E(trans)	2.330(6)	2.561(7)	2.544(11)	2.352(4)
N(1)−C(1)	1.390(9)	1.394(9)	1.40(2)	1.403(5)
Bond Angles (deg)				
N(1)−M−E(cis)	97.7(3)	95.5(3)	98.7(4)	98.1(2)
N(1)−M−E(trans)	169.7(3)	171.4(3)	173.9(4)	169.7(2)
N(1)−M−X(1)	97.8(2)	98.0(2)	95.3(3)	97.01(12)
N(1)−M−X(2)	97.2(2)	97.6(2)	95.1(3)	96.79(11)
N(1)−M−X(3)	100.8(2)	101.4(2)	100.9(3)	100.15(12)
E(cis)−M−E(trans)	72.3(3)	76.0(3)	75.4(4)	71.9(2)
E(cis)−M−X(1)	82.3(2)	86.7(2)	85.8(3)	81.79(9)
E(cis)−M−X(2)	85.9(2)	88.3(2)	90.0(3)	85.88(9)
E(cis)−M−X(3)	161.5(2)	163.0(2)	160.2(3)	161.58(11)
X(1)−M−X(2)	162.00(8)	164.03(7)	169.23(6)	162.65(5)
X(1)−M−X(3)	93.49(10)	88.95(8)	89.37(6)	93.81(5)
X(2)−M−X(3)	93.44(9)	91.46(8)	91.24(6)	94.08(5)
E(trans)−M−X(1)	83.4(2)	80.8(2)	85.6(3)	84.26(9)
E(trans)−M−X(2)	80.1(2)	83.3(2)	83.7(3)	80.32(9)
E(trans)−M−X(3)	89.3(2)	87.1(2)	85.1(3)	89.89(11)
C(1)−N(1)−M	178.1(5)	174.7(6)	176.1(9)	177.7(3)

[a] E(cis) = O(1) (**1** and **7**) or N(2) (**4** and **6**); E(trans) = O(2) (**1** and **7**) or N(3) (**4** and **6**).

(16) Emsley, J. *The Elements*, 2nd ed.; Oxford University Press: New York, 1991.

(17) Clark, G. R.; Glenny, M. W.; Nielson, A. J.; Rickard, C. E. F. *J. Chem. Soc., Dalton Trans.* **1995**, 1147−1152.
(18) Griffith, W. P.; Nielson, A. J.; Taylor, M. J. *J. Chem. Soc., Dalton Trans.* **1988**, 647−649.
(19) Rocklage, S. M.; Schrock, R. R. *J. Am. Chem. Soc.* **1982**, *104*, 3077−3081.
(20) Goeden, G. V.; Haymore, B. L. *Inorg. Chem.* **1983**, *22*, 157−167.
(21) Osborne, J. H.; Trogler, W. C. *Inorg. Chem.* **1985**, *24*, 3098−3099.
(22) Reference 14, Chapter 4.

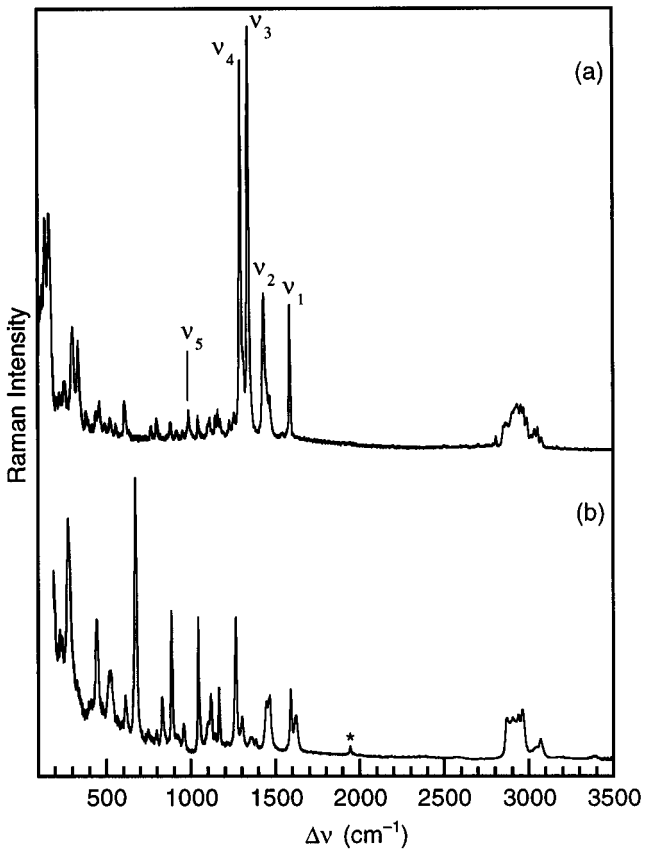

Figure 5. FT-Raman spectra of NAr* compounds, normalized to the ν(C−H) peak intensity (*ca.* 2900 cm^{-1}): (a) Ta(NAr*)Cl$_3$(tmeda) (**4**); (b) H_2NAr*. The peak marked with an asterisk is an artifact.

which the metal and ancillary ligands are systematically varied, allow some detailed vibrational assignments to be made.

Vibrational Modes of the MX_3L_2 Fragment. Three well-separated bands arising from M−X stretching modes are expected for a *mer*-MX_3 unit.[23] The FT-Raman spectra of **1**−**7** contain several obvious candidates for such modes in the low-frequency region (≤600 cm^{-1}). For example, the spectra of the Ta(NAr*)X$_3$(dme) derivatives (Figure 6) exhibit features at 345 (X = Cl (**1**)) and 217 cm^{-1} (X = Br (**5**)) that can be straightforwardly assigned to Ta−X stretches by comparison to established assignments for $[TaX_6]^-$ and $[TaX_6]^{2-}$ (X = Cl, ν = 300−380 cm^{-1}; X = Br, ν = 215−240 cm^{-1}).[24−26] The spectra are complicated by the presence of NAr* bands in the same region, notably at *ca.* 310 and 260 cm^{-1}; thus, weaker M−X features can be unambiguously identified only in difference spectra of pairs of chloride/bromide (**1**/**5**, **4**/**6**) and niobium/tantalum (**1**/**7**) derivatives (*e.g.*, Figure 7). The frequencies of metal−halide bands are given in Table 4. We assign all of the observed features to stretches with the exception of the 160−180 cm^{-1} bands of the chloro derivatives and the 120 cm^{-1} feature of Ta(NAr*)Br$_3$(tmeda) (**6**), which are attributable to metal−halide bending modes.[23] The highest frequency mode for each compound probably involves stretching of the halide trans to L, because this M−X bond is shorter than the others (*vide supra*).

We could not identify bands in the low-frequency region (≤600 cm^{-1}) that are unambiguous candidates for assignment to ν(M−L) modes. Many bands in this region shift as a function of L, but assignments to internal ligand modes are possible for all of them.

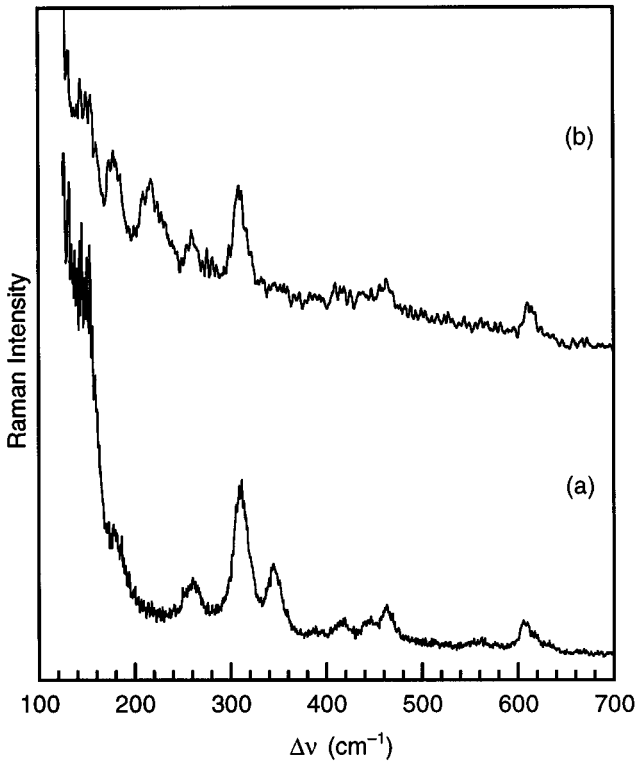

Figure 6. FT-Raman spectra of Ta(NAr*)X$_3$(dme) compounds in the 100−700 cm^{-1} region: (a) Ta(NAr*)Cl$_3$(dme) (**1**); (b) Ta(NAr*)Br$_3$-(dme) (**5**).

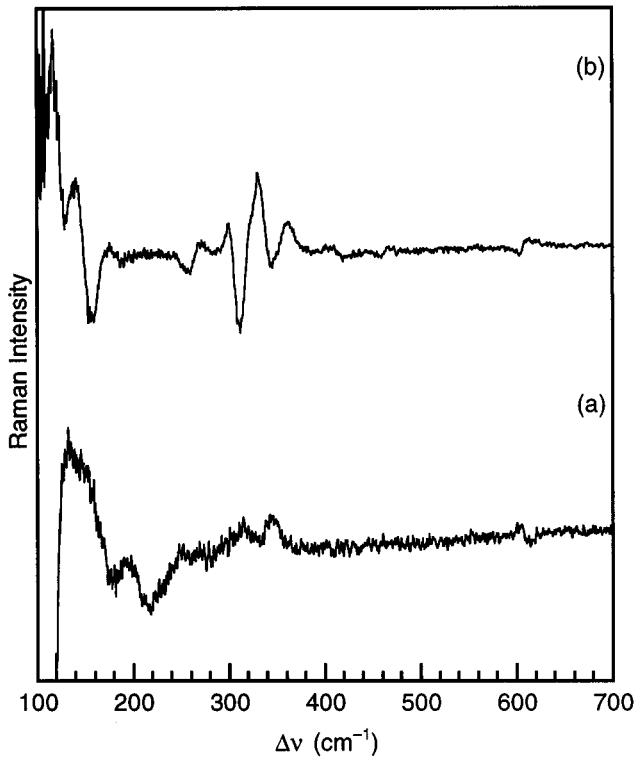

Figure 7. FT-Raman difference spectra of M(NAr*)X$_3$(dme) compounds in the 100−700 cm^{-1} region: (a) Ta(NAr*)Cl$_3$(dme) (**1**) − Ta(NAr*)Br$_3$(dme) (**5**); (b) Nb(NAr*)Cl$_3$(dme) (**7**) − Ta(NAr*)Cl$_3$-(dme) (**1**).

Vibrational Modes of the MNAr* Fragment. "The assignment of the metal−ligand stretching vibrations in both metal−alkylidyne and −organoimido complexes is problematic."[27] The origin of this problem is that the "diatomic"

(23) Nakamoto, K. *Infrared and Raman Spectra of Inorganic and Coordination Compounds*, 4th ed.; Wiley: New York, 1986.
(24) Horner, S. M.; Clark, R. J. H.; Crociani, B.; Copley, D. B.; Horner, W. W.; Collier, F. N.; Tyree, S. Y., Jr. *Inorg. Chem.* **1968**, *7*, 1859−1863.
(25) Brown, D.; Jones, P. J. *J. Chem. Soc. A* **1967**, 247−251.
(26) Brown, T. L.; McDugle, W. G., Jr.; Kent, L. G. *J. Am. Chem. Soc.* **1970**, *92*, 3645−3653.

Table 3. Raman-Vibrational Frequencies (cm^{-1}) for $M(NAr^*)X_3L_2$ Complexes

1	2	3	4	5	6	7	1	2	3	4	5	6	7
151 m sh	146 m	145 m	144 s	153 s	141 m	145 m sh	1161 m	1161 w sh	1161 m	1160 m	1160 m	1161 m	1162 m
			167 s				1177 m		1177 m	1176 w	1177 m	1176 m	1178 m
180 w sh				179 s	182 s	180 w						1196 w	
	191 m						1227 m	1225 m	1230 m	1230 w	1227 m	1229 w	1227 m
					208 s		1259 m	1261 w	1258 m	1257 w	1259 m	1254 m	1260 m
				217 s[a]			1285 w sh				1280 w sh		
			225 vw		223 s		1301 s[b]	1298 s[b]	1303 s[b]	1295 vs[b]	1301 s[b]	1294 vs[b]	1291 vs[b]
260 m	255 w	258 m	257 m	261 m	260 m	268 m		1315 w sh		1311 w sh	1310 w sh	1311 w sh	1311 w sh
					289 w		1357 vs[b]	1353 vs[b]	1356 vs[b]	1341 vs[b]	1353 vs[b]	1341 vs[b]	1334 vs[b]
311 s	306 s	309 s	305 s	311 s	309 s	303 s						1365 vw sh	1363 w sh
						322 m	1385 w sh					1387 vw	1386 w
345 m[a]	337 m[a]	336 m[a]	338 s[a]			331 s[a]	1433 s[b]	1432 s[b]	1435 s[b]	1433 s[b]	1431 s[b]	1432 s[b]	1427 s[b]
					346 w sh	348 m	1460 m sh	1460 w sh	1464 w sh	1448 w sh	1455 m sh	1456 m	1458 m
						360 w sh[a]				1469 m		1469 m	
388 w			385 w		387 w			1490 w	1486 w sh				
416 m				420 w		412 w	1538 vw		1548 w	1541 w		1535 vw	1541 vw
444 m	444 m	446 m	443 w	441 w	446 m	445 w						1560 vw	
464 m	460 m	464 m	461 m	464 m	464 m	465 m		1572 w sh					
			495 vw		493 w		1586 s[b]	1588 s[b]	1587 s[b]	1586 s[b]	1587 s[b]	1585 s[b]	1585 s[b]
			525 w		531 w		1615 vw	1608 w				1610 vw	1625 vw sh
558 w			556 w		559 w	557 w						1648 w	
608 m	610 m	613 m	610 m	615 m	611 m	610 m	1663 vw		1662 w	1675 vw			
618 w sh						618 vw sh						1696 w	
633 w sh	632 w		635 vw			633 w				2808 w		2806 w	
	651 w						2851 w			2852 w		2850 w	2850 w
		672 vw		670 w		671 vw	2867 w	2867 w	2871 w	2866 w	2863 w	2866 w	2867 w
730 w		728 vw		730 w	729 w	730 w				2876 m			
764 w		770 w	766 w	765 w	766 w	765 w	2906 w sh	2902 w	2907 w	2905 m	2906 w sh	2903 m	2907 w sh
			799 w		800 m					2920 w sh			
810 vw						811 w	2926 w sh	2931 w	2935 w	2934 m	2925 w sh	2929 m	2929 w sh
858 m		856 m		855 m		858 m	2947 m		2954 w	2955 m	2945 m	2950 w sh	2945 m
886 m	885 w	884 m	881 w	885 m	884 m	886 m	2966 w sh				2963 w sh	2965 m	2965 w
			917 w		916 w		2973 m	2969 w	2975 w	2971 m	2972 w		2978 w
		928 m					2996 vw sh			2991 m	2994 vw sh	2981 w	2995 vw sh
958 w		958 w	954 w		953 w	959 w				3014 w			
			976 vw sh		976 w sh				3019 w			3021 w	3026 vw
998 m[b]	993 m[b]	997 m[b]	989 m[b]	998 m[b]	990 m[b]	993 m[b]				3037 w			
	1013 s												3046 vw
1024 vw		1023 vw		1020 vw			3051 vw sh	3052 w	3055 w	3054 w	3057 w	3050 w	
1046 m	1046 m	1047 m	1045 m	1046 m	1044 m	1046 m	3060 w						3060 w
					1065 vw sh			3065 w					
1082 w				1082 w		1082 w	3075 w sh	3071 w		3077 w	3073 w		3074 w
			1102 w sh					3084 w					
1110 m	1113 w	1111 m	1113 w	1110 m	1110 m	1112 m		3142 vw					3135 vw
			1126 vw		1125 vw	1123 vw sh	3170 vw		3176 vw	3171 vw	3176 vw	3167 vw	3169 vw
1147 m	1146 w	1147 m	1147 w	1147 m	1147 m	1146 m							

[a] M−X mode; see Table 4 and associated discussion for assignment. [b] MNAr* mode; see Table 5 and associated discussion for assignment.

Table 4. Vibrational Frequencies (cm^{-1}) of M−X Modes for $M(NAr^*)X_3L_2$ Complexes

1	2	3	4	5	6	7
345 m	337 m	336 m	338 s	217 s	222[a]	360 w sh
315[a]			300[a]		208[a]	331 s
258[a]				180[a]		272[a]
158[a]			168[a]		120[a]	175[a]

[a] Frequency is from difference spectrum or spectra; features are obscured by other bands in raw spectrum.

stretching frequencies of M≡N bonds (1000−1100 cm^{-1}) are similar to N−C stretching frequencies (*e.g.*, 1279 cm^{-1} for aniline),[28] so the two stretches in the linear M≡N−C unit (ignoring, for the moment, the substituents on the carbon atom) are expected to couple very strongly to produce symmetric and asymmetric ν(MNC) modes that are shifted to higher and lower frequencies of the average of the M≡N and N−C stretching frequencies.[29,30] Two bands that shift on ^{15}N labeling have been located in the vibrational spectra of mono(arylimido)metal complexes[18−21] at 1330−1360 cm^{-1} ($\Delta\nu(^{14}N/^{15}N)$ = 15−30 cm^{-1}) and 930−1020 cm^{-1} ($\Delta\nu(^{14}N/^{15}N)$ = 5−15 cm^{-1}). As has been noted by others,[18] neither band can be assigned to ν(M≡N) because the calculated $^{14}N/^{15}N$ isotopic shift for the ν(M≡N) oscillator (*ca.* 40 cm^{-1}) is substantially larger than either of the observed shifts; mixing between ν(M≡N) and ν(N−C) is significant.[31]

In terms of identifying the Raman bands of **1**−**7** that arise from modes containing appreciable ν(M≡N) character, it is reasonable to expect that the frequencies and intensities of such bands will exhibit a strong dependence on the nature (or absence) of the metal atom. Comparisons of the Raman spectra of **1**−**7** to that of the free, protonated ligand (H_2NAr^*) reveal that correspondences in frequencies are, in general, not close outside the ν(CH) region (Figure 5), so this particular comparison is not especially informative. However, there is a striking difference between the intensities of four features in the 1100−1700 cm^{-1} range, which are greatly intensified for the metal compounds relative to the bands of H_2NAr^* in this region. These four intense bands, which we denote ν_1 through ν_4, are identified in Figure 5, and their frequencies are given in Table 5.

A comparison of the spectrum of $Nb(NAr^*)Cl_3$(dme) (**7**) to that of $Ta(NAr^*)Cl_3$(dme) (**1**) (Figure 8) reveals that three of the four anomalously intense bands (ν_2, ν_3, ν_4) exhibit large frequency shifts with the change in metal atom ($\Delta\nu$(Nb/Ta) = 6−23 cm^{-1}, Table 5). Aside from these, there is only one other band above 400 cm^{-1} that shifts significantly upon metal substitution; this band, at 993 cm^{-1} for **7** and 998 cm^{-1} for **1**, is denoted ν_5 (Figure 8) and is included in Table 5. The effects of ancillary ligand variation on ν_1 and ν_2 are negligible ($\Delta\nu \leq$ 4 cm^{-1}); only ν_3, ν_4, and ν_5 exhibit appreciable shifts ($\Delta\nu$ = 9−16 cm^{-1}, Table 5), with the tmeda compounds $Ta(NAr^*)X_3$(tmeda) (X = Cl (**4**), Br(**6**)) exhibiting lower frequencies than the dme, thf, and py derivatives.

On the basis of prior studies on related metal−arylimido compounds, ν_3 and ν_5 can be assigned to modes with significant ν(M≡N) character. Specifically, Rocklage and Schrock reported that the infrared spectrum of $Ta(NPh)Cl_3(thf)_2$ exhibits a band at 1360 cm^{-1} that shifts 25 cm^{-1} upon ^{15}N labeling of the imido ligand;[19] this band almost exactly coincides with ν_3 for closely related $Ta(NAr^*)Cl_3(thf)_2$ (**3**) (1356 cm^{-1}) and with those of the other $M(NAr^*)X_3L_2$ derivatives (M = Ta, 1341−1357 cm^{-1}; M = Nb, 1334 cm^{-1}; Table 5). In addition, Griffith and co-workers reported[18] that the Raman spectra of tungsten−phenylimido complexes exhibit five bands that are closely analogous to ν_1−ν_5 of **1**−**7**, except that their equivalent of ν_4 is both lower in frequency (1170 vs 1300 cm^{-1}) and less intense (*vide infra*). The bands corresponding to ν_3 and ν_5 exhibit large shifts upon ^{15}N labeling and were assigned as ν_{sym}(WNC) and ν_{asym}(WNC); in contrast, ^{15}N labeling had little effect ($\Delta\nu(^{14}N/^{15}N) \leq 2$ cm^{-1}) on the analogues of ν_1, ν_2, and ν_4.[32]

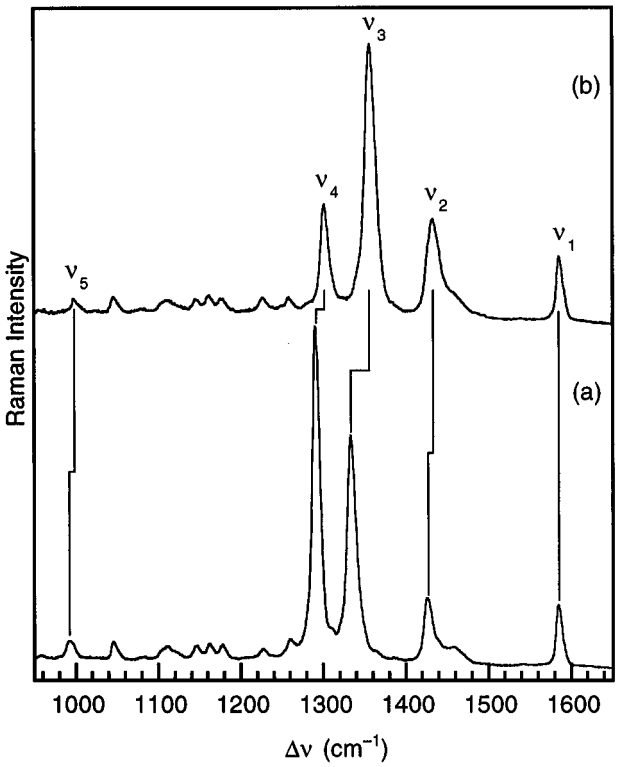

Figure 8. FT-Raman spectra of $M(NAr^*)Cl_3$(dme) compounds in the 1200−1700 cm^{-1} region: (a) $Nb(NAr^*)Cl_3$(dme) (**7**); (b) $Ta(NAr^*)Cl_3$(dme) (**1**).

A general problem with describing the "ν(MNC)" modes of metal−arylimido complexes as being nominal symmetric and antisymmetric combinations of ν(M≡N) and ν(N−C) is that the N−C stretching mode of aniline is not a localized single-bond stretch. Varsányi correlated "ν(N−C)" of aniline to benzene mode 13 (Figure 9)[28,33−35] but noted that C−X stretching modes of C_6H_5X compounds are generally also mixed

(27) Reference 14, p 123.
(28) Varsányi, G. *Vibrational Spectra of Benzene Derivatives*; Academic Press: New York, 1969.
(29) Dehnicke, K.; Strähle, J. *Angew. Chem., Int. Ed. Engl.* **1981**, *20*, 413−426.
(30) Dehnicke, K.; Strähle, J. *Chem. Rev.* **1993**, *93*, 981−994.
(31) Osborne and Trogler[21] have argued that the 1350-cm^{-1} band can be assigned to ν(C−N) because the $^{14}N/^{15}N$ frequency shift is close to that calculated for a C−N diatomic oscillator. However, this calculation does not take account of the fact that the metal atom must be assumed to "ride" on the N atom if mixing with ν(M≡N) is ignored, as it is in a diatomic ν(C−N) calculation; this greatly reduces the calculated $^{14}N/^{15}N$ isotopic shift.
(32) Griffith et al.[18] observed a third $^{14}N/^{15}N$-sensitive band at *ca.* 680 cm^{-1} in the Raman spectra of tungsten−phenylimido compounds, for which they suggested assignment to the δ(W≡N−C) bending mode. There are several weak Raman and infrared bands in the 600−800 cm^{-1} region of **1**−**7** that might be analogues of this band, but ^{15}N data would be required to establish this correlation. We note, however, that data for other X≡Y−Ph compounds suggest that 680 cm^{-1} is implausibly high for a δ(M≡N−C) mode. For example, the δ(Cr≡C−C) mode of *trans*-Cr(≡CCH_3)$(CO)_4$Br (Foulet-Fonseca, G. P.; Jouan, M.; Dao, N. Q.; Fischer, H.; Schmid, J.; Fischer, E. O. *Spectrochim. Acta* **1990**, *46A*, 339−354) has been assigned at 356 cm^{-1} and the δ(C≡N−C) modes of C_6H_5N≡C[38] are assigned at 325 cm^{-1} (in-plane component) and 478/162 cm^{-1} (out-of-plane component, strongly mixed with the Ph−NC wag). Alternative assignments for the 680 cm^{-1} band of tungsten−phenylimido complexes are to benzene mode 1 or 6a (*vide infra*), either of which could plausibly possess substantial ν_{sym}(W≡N−C) character.
(33) Varsányi, G. *Assignments for Vibrational Spectra of Seven Hundred Benzene Derivatives*; Wiley: New York, 1974.

Table 5. Vibrational Frequencies (cm^{-1}) of $M(NAr^*)X_3L_2$ Complexes Relevant to $\nu(M{\equiv}N)$

band	assignt[a]	**1**	**2**	**3**	**4**	**5**	**6**	**7**
ν_1	8a	1586 s	1588 s	1587 s	1586 s	1587 s	1585 s	1585 s
ν_2	19a	1433 s	1432 s	1435 s	1433 s	1431 s	1432 s	1427 s
ν_3	$\nu(M{\equiv}N)-13$	1357 vs	1353 vs	1356 vs	1341 vs	1353 vs	1341 vs	1334 vs
ν_4	9a	1301 s	1298 s	1303 s	1295 vs	1301 s	1294 vs	1291 vs
ν_5	$\nu(M{\equiv}N)+13$	998 m	993 m	997 m	989 m	998 m	990 m	993 m

[a] See Figure 9.

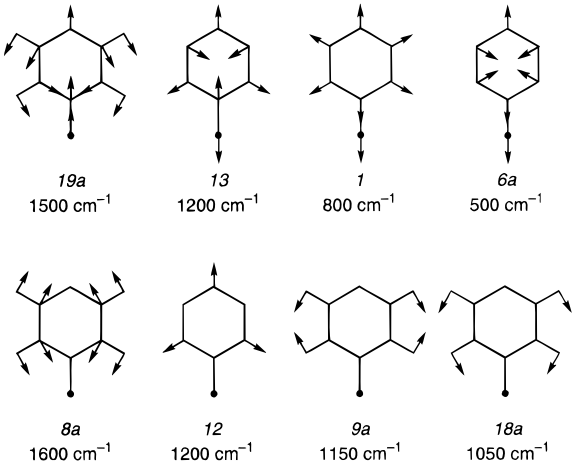

Figure 9. Symmetric vibrational modes of C_6H_5X for "light" X, following Varsányi.[33] Modes with significant C−H stretching character are excluded. Varsányi's labels (in italics) and approximate, characteristic frequencies for each mode are noted. The modes in each row are ordered according to frequency; those in the top row contain some ν(C−X) character.

with other benzene modes. Thus, at minimum, modes ν_3 and ν_5 should be described as the asymmetric and symmetric combinations $\nu(M{\equiv}N)-13$ and $\nu(M{\equiv}N)+13$, respectively.[36]

The implication of the strongly mixed character of ν(N−C) for metal−arylimido compounds is that the interaction between this oscillator and $\nu(M{\equiv}N)$ will affect the other modes with which ν(N−C) is mixed. For **1**−**7** this is manifested by the fact that, in addition to ν_3 and ν_5, bands ν_2 and ν_4 are also sensitive to the nature of the metal atom (Figure 8), exhibiting frequency shifts (ν_2 1433 (**1**), 1427 cm^{-1} (**7**); ν_4 1301 (**1**), 1291 cm^{-1} (**7**)) that parallel that of ν_3 (1357 (**1**), 1334 cm^{-1} (**7**)); this suggests that the modes that give rise to these bands are strongly mixed. While the analogues of ν_2 and ν_4 in the Raman spectra of tungsten−phenylimido complexes[18] do not shift upon ^{15}N substitution, a key difference between ^{15}N-isotopic substitution and metal atom substitution is that the former only affects vibrational frequencies via mass (kinematic) effects in the **G** matrix—that is, vibrational modes are affected solely to the extent that they involve center-of-mass motion of the nitrogen atom—whereas metal atom substitution can also affect frequencies through the **F** matrix (force constants).[35] The consequences of **F**-matrix changes can be different from ^{15}N-induced **G**-matrix changes in that rediagonalization can occur in modes that do not involve significant N atom motion.[37]

Candidates for C_6H_5X modes that could mix with $\nu(M{\equiv}N)$ are those that are totally symmetric in the local C_{2v} symmetry of the MNAr* fragment; excluding ν(CH) modes and mode 13, these are modes 1, 6a, 8a, 9a, 12, 18a and 19a (Figure 9). Of these, modes 1 and 6a can be excluded because they are energy-factored from $\nu(M{\equiv}N)$ and modes 8a and 12 are excluded because the forms of their displacements contain little C−X character.[33,38] Mode 19a, however, has been found to mix appreciably with ν(C−X) for compounds such as $C_6H_5C{\equiv}P$[38] and exhibits a frequency of *ca.* 1500 cm^{-1} in simple C_6H_5X derivatives; thus, ν_2 is assigned to mode 19a. Modes 9a and 18a are primarily C−H bending;[33] the analogue of ν_4 in the Raman spectra of tungsten−phenylimido complexes[18] has a frequency (*ca.* 1170 cm^{-1}) consistent with assignment to 9a. It is known that 2,6-dialkylation strongly perturbs these bending modes relative to those of simple benzene derivatives; ν_4 of **1**−**7** presumably correlates to such a bending mode, although, as discussed by Varsányi,[33] such correlations are neither straightforward nor unique.

The fifth intense band, ν_1, does not shift with metal substitution in **1**−**7**, and analogous bands for related compounds are insensitive to ^{15}N labeling of the imido ligand. On the basis of these properties and its characteristic frequency of *ca.* 1600 cm^{-1}, ν_1 can be straightforwardly assigned to Ar*-localized mode 8a (Figure 9).[39]

With these assignments of bands $\nu_1-\nu_5$ in hand, it remains to address the observations that $\nu_1-\nu_4$ exhibit strong Raman intensities and that ν_5 does not. An explanation that is self-

(34) We have adopted Varsányi's notation for labeling the vibrational modes of C_6H_5X derivatives with "light" X substituents,[33] which is based upon that for benzene,[35] for the sake of consistency with the extensive studies by Dao, Fischer, and co-workers on $M(\equiv CPh)(CO)_4X$ (X = halide) complexes (Dao, N. Q.; Fischer, E. O.; Kappenstein, C. *Nouv. J. Chim.* **1980**, *4*, 85−94 and references therein). Correlations to the alternative mode labeling scheme of Tasumi et al. (Tasumi, M.; Urano, T.; Nakata, M. *J. Mol. Struct.* **1986**, *146*, 383−396) are as follows: $1 = R_5^{ip}$; $6a = R_{6a}^{ip}$; $8a = R_{1a}^{ip}$; $9a = HB_{2a}^{ip}$; $12 = R_4^{ip}$; 13 = C−X; $18a = HB_{4a}^{ip}$; $19a = R_{2a}^{ip}$. Modes 1, 6a, and 13 correspond to Whiffen's X-sensitive modes r, t, and q, respectively (Whiffen, D. H. *J. Chem. Soc.* **1956**, 1350−1356).

(35) Wilson, E. B., Jr.; Decius, J. C.; Cross, R. G. *Molecular Vibrations*; McGraw-Hill: New York, 1955.

(36) We differ here from Griffith and co-workers,[18] who explicitly assigned ν_3 to the symmetric $\nu(M{\equiv}N-C)$ mode. Valence force-field calculations on the general model system W−A−B (Miskowski, V. M.; Hopkins, M. D. Unpublished results) in which the two stretching force constants and the masses of A and B are continuously varied show unambiguously that the higher frequency of the two ν(MNC) modes must be the asymmetric one, in agreement with the qualitative arguments put forth by Dehnicke and Strähle.[29] Because both the symmetric and antisymmetric ν(MNC) modes transform as A_1 in the local C_{2v} symmetry of the MNAr oscillator, Raman depolarization ratios[18] cannot distinguish between them. We lack sufficient vibrational data (*e.g.*, for ^{15}N and ^{13}C isotopomers) to allow refinement of a full force field for the present compounds.

(37) The effect of niobium-for-tantalum substitution on the reduced mass of a diatomic $M{\equiv}N$ oscillator is very similar to the effect of ^{15}N substitution but results in a shift in frequency opposite to that observed for $Ta(NAr^*)Cl_3(dme)$ (**1**) and $Nb(NAr^*)Cl_3(dme)$ (**7**). This indicates that the primary origin of the observed shifts is that the $M{\equiv}N$ force constant is larger for tantalum than for niobium. This ordering of force constants is contrary to that expected from the $M{\equiv}N$ bond distances for $Nb(NAr^*)Cl_3(dme)$ and $Ta(NAr^*)Cl_3(dme)$, but comparisons of $M{\equiv}E$ bond distances and stretching frequencies for other pairs of analogous $M(E)L_n$ complexes of second- and third-transition-series metals[14,22] reveal numerous examples of third-row compounds with simultaneously longer bond distances and higher stretching frequencies than those of their second-row counterparts. Two unambiguous examples of this phenomenon are $[AsPh_4][M(\equiv N)Cl_4]$ ($d(Ru{\equiv}N)$ = 1.570(7) Å, $\nu(Ru{\equiv}N)$ = 1092 cm^{-1}; $d(Os{\equiv}N)$ = 1.604(10) Å, $\nu(Os{\equiv}N)$ = 1123 cm^{-1}: Collin, A. J.; Griffith, W. P.; Pawson, D. *J. Mol. Struct.* **1973**, *19*, 531−544. Phillips, F. L.; Skapski, A. C. *J. Cryst. Mol. Struct.* **1975**, *5*, 83−92. Phillips, F. L.; Skapski, A. C. *Acta Crystallogr.* **1975**, *B31*, 2667−2670) and $M(\equiv O)Cl_4$ ($d(Mo{\equiv}O)$ = 1.658(5) Å, $\nu(Mo{\equiv}O)$ = 1015 cm^{-1}; $d(W{\equiv}O)$ = 1.686(11) Å, $\nu(W{\equiv}O)$ = 1027 cm^{-1}: Fijima, K.; Shibata, S. *Bull. Chem. Soc. Jpn.* **1975**, *48*, 666−668. Fijima, K.; Shibata, S. *Bull. Chem. Soc. Jpn.* **1974**, *47*, 1393−1395).

(38) Ohno, K.; Matsuura, H. *J. Mol. Struct.* **1991**, *242*, 303−314.

consistent with their mode assignments is that $\nu_1-\nu_4$ exhibit preresonance enhancement from a [π(M≡NAr*) → π*-(M≡NAr*)] electronic transition. The electronic-absorption spectra of **1**−**7** contain a strong, near-UV band (band II, $\lambda_{max} \cong 300$ nm, $\epsilon_{max} \cong 10^4$ M^{-1} cm^{-1})[1] that can be logically assigned to this fully allowed transition.[40] That preresonant enhancement can be significant this far from resonance (20 000 cm^{-1}) for an intense electronic transition is well established.[41−43] The M≡N bond length should dramatically increase in the [π(M≡NAr*) → π*(M≡NAr*)] excited state because the M−N bond order is reduced from (formally) 3 to 2; the N−C and internal Ar* bond lengths should also change in the excited state, with the extent of these distortions depending upon the degree to which the M≡N and Ar* π/π* systems are conjugated.

The preresonant enhancement of ν_3 from the [π(M≡NAr*) → π*(M≡NAr*)] transition, and lack thereof for ν_5, likely reflects the nature of the ν(MNC) contributions to these modes. The form of ν_3 (ν(M≡N)−13) is essentially an oscillation of the nitrogen atom between the relatively massive metal center and Ar* group; hence, it involves a large M≡N distortion. In contrast, ν_5 (ν(M≡N)+13) consists of a symmetric combination of M≡N and N−C displacements; the larger mass of M dictates that nuclear motion along the N−C coordinate will be larger than that along M≡N. The enhancement of ν_2 and of ν_4 similarly reflects the relative contribution of ν(M≡N) to these modes. It is noteworthy that the intensity of ν_4 decreases as the energy separation from ν_3 increases upon tantalum-for-niobium substitution (Figure 8), presumably reflecting a corresponding decrease in the ν(M≡N) character of ν_4 as mixing decreases; the fact that ν_4 in tungsten−phenylimido complexes[18] is simultaneously lower in frequency and much weaker than for **1**−**7** may be a continuation of this trend. The enhanced intensity of ν_1, which has relatively little ground-state ν(M≡N) character, is reasonable if π*(Ar*)/π*(M≡N) conjugation is significant because this symmetric benzenoid mode will make an important contribution to excited-state distortion.

Implications for Luminescence Properties of M(NAr*)-X_3L_2 Compounds. The structural and Raman-spectroscopic results described herein for **1**−**7** are consistent with the bonding description inferred from their electronic spectra.[1] We previously reported that the [π(M≡NAr*) → d_{xy}] absorption and [π(M≡NAr*) ← d_{xy}] emission band maxima of tantalum compounds **1**−**6** shift over relatively small ranges as functions of X and L ($\bar{\nu}^{abs}_{max} = 19275-22450$ cm^{-1}; $\bar{\nu}^{em}_{max} = 13550-15550$ cm^{-1}),[1] which suggests that the structures of their MNAr* units are insensitive to ligand substitution. In agreement with this, the X-ray crystal structures for tantalum derivatives **1**, **4**, and **6** reveal that the bond distances and angles of the MNAr* fragments are essentially independent of X and L, and the Raman frequencies of MNAr* modes $\nu_1-\nu_5$ exhibit relatively small variations upon ligand substitution among compounds **1**−**6**. Unless ligands capable of inducing larger electronic or structural perturbations are employed, it is likely, then, that the best means of controlling the energy of the emissive state are metal[1] and imido R group[2] substitution.

The more important implications of the natures of X and L for the photophysical properties of **1**−**7** are that they exert substantial influence over the nonradiative decay rate and, thus, over the emission lifetimes and quantum yields. The present results do not yield significant insight into the complex factors that underlie this control of the nonradiative decay rate. Complementary photophysical and vibrational-spectroscopic data for compounds in which Ar* and L are selectively isotopically labeled will be required to probe this point.

The Raman-spectroscopic assignments are important for understanding our earlier observation that the [π(M≡NAr*) ← d_{xy}] emission spectra of **1**−**7** exhibit a 1000−1100 cm^{-1} vibronic progression at 13 K.[1] We suggested that this progression arises from an MNAr* mode (or unresolved set of MNAr* modes) with significant ν(M≡N) character because the M≡N bond order decreases from 3 to $2^1/_2$ in the excited state. The present data provide four MNAr* modes with appreciable ν(M≡N) character in the 900−1450 cm^{-1} region ($\nu_2-\nu_5$) that could give rise to or contribute strongly to this progression. The broad line widths of the emission spectra and the fact that the observed vibronic frequencies do not match the Raman frequencies of modes $\nu_2-\nu_5$ suggest that the emission spectra exhibit a composite progression with a frequency that is an intensity-weighted average of those of its constituent modes. Unfortunately, the relative intensities of the Raman bands cannot necessarily be taken to represent their likely relative contribution to the emission progression because they result from preresonant enhancement with a [π(M≡NAr*) → π*(M≡NAr*)] transition, with which should be associated a significantly different excited-state structural distortion than that for the emissive [π(M≡NAr*) → d_{xy}] state. Nonetheless, we expect that mode ν_3 contributes particularly strongly to the progression, given the large M≡N motion in this vibration.

Acknowledgment. This research was supported by National Science Foundation Grant CHE 9307013.

Supporting Information Available: CIF printouts and ORTEP plots showing complete atomic labeling for Ta(NAr*)Cl_3(dme) (**1**), Ta(NAr*)Cl_3(tmeda) (**4**), Ta(NAr*)Br_3(tmeda) (**6**), and Nb(NAr*)Cl_3(dme) (**7**) (32 pages). Ordering information is given on any current masthead page.

IC970494+

(39) After this paper was submitted for publication, Williams and co-workers (Korolev, A. V.; Rheingold, A. L.; Williams, D. S. *Inorg. Chem.* **1997**, *36*, 2647−2665) reported an analysis of the MNR vibrational modes of related niobium and tantalum alkyl- and arylimido compounds (based on "visual inspection of animated vibrational modes" generated by the Spartan computation package) that is in general agreement with this and prior work with respect to the conclusion that the MN and NC stretching modes couple to yield symmetric and antisymmetric combinations that are mixed further with internal R group modes. Such mixing is, of course, extremely R group dependent, and, thus, the present results do not directly bear on their findings for alkylimido compounds. We note, however, that the assignment by Williams and co-workers of an infrared band in the range 1585−1610-cm^{-1} for M(NAr)Cl_3(dme) (M = Nb, Ta; Ar = Ph, Ar*) as the "(mainly) N−C mode" is at odds with our assignment of the strong Raman band in this region to the aryl-localized mode 8a. The modes with appreciable N−C character will lie at much lower frequency, as described in the text.

(40) The [π(M≡NAr*) → π*(M≡NAr*)] transition was not assigned in our earlier paper, but the observed lack of dependence of the transition energy on X and L is consistent with such an assignment. The low intensity of the [π(M≡NAr*) → d_{xy}] absorption band ($\lambda_{max} \cong 500$ nm, $\epsilon_{max} \cong 10^2$ M^{-1} cm^{-1}) precludes it from providing significant Raman-intensity enhancement, even at resonance. Raman spectra for **1**−**7** using visible excitation ($\lambda_{ex} = 632.8$ nm) were of significantly lower quality than those reported here due to photodecomposition of the samples, but the intense bands $\nu_1-\nu_4$ were nonetheless evident in the spectra (Dallinger, R. F. Unpublished results).

(41) Myers, A. B. In *Laser Techniques in Chemistry*; Myers, A. B., Rizzo, T. R., Ed.; Wiley: New York, 1995; pp 325−384.

(42) Miskowski, V. M.; Smith, T. P.; Loehr, T. M.; Gray, H. B. *J. Am. Chem. Soc.* **1985**, *107*, 7925−7934.

(43) Quicksall, C. O.; Spiro, T. G. *Inorg. Chem.* **1970**, *9*, 1045−1049.